Medical Engineering and Physics 64 (2019) 65–73

Contents lists available at ScienceDirect

Medical Engineering and Physics

journal homepage: www.elsevier.com/locate/medengphy

Assessing the feasibility of adaptive planning for prostate radiotherapy using Smartadapt deformable image registration

Virginia Marin Anaya [a,*], Jamie Fairfoul [b]

[a] Medical Physics Department, Biomedical Campus, Cambridge University Hospitals NHS Foundation Trust, Addenbrooke's Hospital, Hills Road, Cambridge CB2 0QQ, United Kingdom

[b] Radiotherapy Department, North West Anglia NHS Foundation Trust, Peterborough City Hospital, Edith Cavell Campus, Bretton Gate, Peterborough PE3 9GZ, United Kingdom

ARTICLE INFO

Article history:
Received 18 December 2017
Revised 7 January 2019
Accepted 8 January 2019

Keywords:
Adaptive planning
Deformable image registration
Prostate
Cone-beam CT

ABSTRACT

Background: The purpose of this study is to assess the feasibility of adaptive planning for prostate cancer using SmartAdapt deformable image registration (DIR), in an effort to reduce the effect of patient-specific variations.

Methods: 18 prostate patients (74 Gy in 37 fractions) were selected. Each patient had a planning CT and cone-beam CT (CBCT) images acquired at different fractions. For each fraction, the planning CT was registered to the CBCT image dataset using SmartAdapt. A rigid registration was performed prior to the DIR. The manual contours on the CBCT images by the clinician were used as reference. For the geometric analysis, various evaluation metrics were used to compare the volumes for both rigid and DIR. For the dosimetric analysis, the initial treatment plan was recalculated on the smartadapted structures, using Eclipse. Several Dose-Volume Histogram (DVH) points were used for the evaluation.

Results: The results of the geometric analysis indicate that DIR can result in worse evaluation metrics than rigid registration alone. In general, SmartAdapt tends to under-contour the volumes. The difference in DVH points between the deformed and the reference prostate was worse than the difference between the planning CT and the reference, overestimating the need for re-planning. However, there was a tendency for the deformed rectum to underestimate the need for re-planning.

Conclusions: After cautious analysis of the results, it has been decided not to implement SmartAdapt clinically to trigger adaptive decisions

1. Introduction

Prostate cancer is the most common cancer affecting men in the UK [1]. According to Cancer Research UK statistics, 1 in 8 men will be diagnosed with prostate cancer during their lifetime [2]. External beam radiotherapy is one treatment option available to patients. In our department, RapidArc, which is the Varian implementation of volumetric modulated arc therapy (VMAT) developed by Otto [3], is used to treat prostate patients. However, prostate cancer presents several challenges such as inter-and intra-fractional variations in patient set-up and anatomy. At our hospital, online image-guided radiotherapy (IGRT) is being used for prostate patients to correct the translational inter-fractional motion at each fraction. All prostate patients receive daily online IGRT with kV cone-beam CT (CBCT) for prostate to prostate soft tissue matching (without fiducials). The use of CBCT allows the localisation of the target and organs at risk in the treatment position before treatment delivery, which enables online correction by comparing CBCT images with the CT planning images [4,5]. Although soft-tissue matching without fiducials is a non-invasive procedure, it is subjective, time-consuming and suffers from inter-and intra-observer variability. SmartAdapt deformable image registration (DIR) has the potential of being a useful tool in adaptive radiotherapy to account for anatomical changes during the course of radiotherapy treatment.

The aim of this study is to assess the feasibility of adaptive planning for prostate RapidArc using the Varian SmartAdapt Version 11 DIR tool, in an effort to reduce the effect of patient-specific variations. SmartAdapt consists of a rigid registration framework and a deformable algorithm. The DIR algorithm in SmartAdapt is based on the Demons algorithm introduced by Thirion in 1998 [6]. The Demons algorithm uses intensity differences between the source and the target images as well as gradient information from the source image to determine the force necessary to deform the target image. The model assumes that there are "demons"

* Corresponding author.
E-mail addresses: virginia.marinanaya1@nhs.net (V. Marin Anaya), jamie.faifoul@nhs.net (J. Fairfoul).

https://doi.org/10.1016/j.medengphy.2019.01.001
1350-4533/

applying forces that push or pull the voxels of the target image to match the source image as closely as possible [7]. The model also assumes that the boundaries of objects in one image are semi-permeable membranes and the other image diffuses through these membranes by the action of the “demons” situated within the membranes. The Demons algorithm treats the deformation as a diffusion process, governed by a diffusion equation. The diffusion equation is then solved iteratively by adding incremental changes in the position of voxels in the target image so that the source image can be brought voxel by voxel into spatial alignment with the target image. In our study, the source image is the treatment planning CT and the target image is the CBCT image, which contains information about anatomical changes from the initial planning CT image. The result of the DIR is a deformation vector field that can be used to deform the contours specified in the initial planning CT to match the CBCT image. The contours in the volume of interest from the initial planning CT can be propagated onto the CBCT image. Once the DIR is completed, the contours will be automatically delineated in the CBCT image. The ideal result of the DIR is a new image dataset with the image quality of the CT and the anatomical information of the CBCT image. The reader is referred to the literature [6–8] for more technical details on the Demons algorithm.

To date, most studies that evaluate the performance of SmartAdapt or other DIR algorithms are limited to head and neck such as Eiland et al. [9], Veiga et al. [10], and Tsuji et al. [11]. Some studies only perform a geometrical analysis, such as Hou et al. [12]. Moreover, due to the need for manually-drawn contours by the clinician (reference), most studies are limited to small numbers of patients. Furthermore, some studies [13] compare the new treatment plan, using the deformed image dataset and the same settings as in the original plan, with the initial treatment plan to assess the dosimetric impact of inter-fractional organ deformation. Although this method is useful for investigating the dosimetric impact of organ deformation between fractions, it fails to assess the feasibility of using SmartAdapt clinically to trigger adaptive decisions because the method does not have a reference or gold standard. To our knowledge the method used for the dosimetric analysis in our study is novel and allows the comparison of the absorbed doses to the prostate and rectum between the original planning, the deformed and the reference volumes/structures.

The study has been divided into two parts. The first part consists of a geometric evaluation of the deformed volumes/structures generated by SmartAdapt compared with the manual contours produced by the clinical oncologist on CBCT images, which will be considered the reference or gold standard. Several evaluation metrics will be used to quantify the agreement between contours. The second part consists of a dosimetric evaluation, where the initial treatment plan will be re-calculated on the smartadapted volumes/structures, using Eclipse. Several Dose-Volume Histogram (DVH) points and the Conformity Index (CI) will be used for the evaluation. Analysis of the geometric and dosimetric results will be performed to assess the usefulness of SmartAdapt in adaptive planning for prostate RapidArc. The results, including the strengths and limitations of the methods used, will be discussed and compared with other studies in the literature.

2. Methods

Fig. 1 shows an overview of the methods used in this study.

18 prostate cancer patients treated in 37 fractions using RapidArc with a prescribed dose of 74 Gy (2 Gy per fraction) were selected to evaluate the performance of Varian SmartAdapt version 11. Each patient had a planning CT and CBCT images acquired on each treatment fraction. CBCTs from fractions 1, 6, 11, 16, 21, 26, and 31 had the prostate and rectum re-outlined.

The reader is referred to previous publication by Maund et al. [14] for boxplots showing the variation in rectal volume on CBCT images during treatment for these 18 patients and a bar graph illustrating the change in rectal volume on CBCT relative to the original planning CT scan volume, which highlights the challenges present in prostate radiotherapy.

For the initial planning CT scan and in accordance with clinical protocol, all the patients were given information on diet to minimise flatus and regulate rectal filling and drinking protocols to follow. All the patients were imaged supine on the flat CT couch with their heads supported using a headrest and their arms resting on their chests. Their legs were immobilised using knee supports and ankle stocks.

Manual delineations of target volumes and organs at risks on the non-contrast enhanced planning CT images were performed by the clinician using Prosoma virtual simulation software (Medcom GmbH, Darmstadt, Germany). The CTV1 (prostate and seminal vesicles) and the CTV2 (prostate only) were contoured on the planning CT images with a 2 mm slice thickness. A 10 mm margin

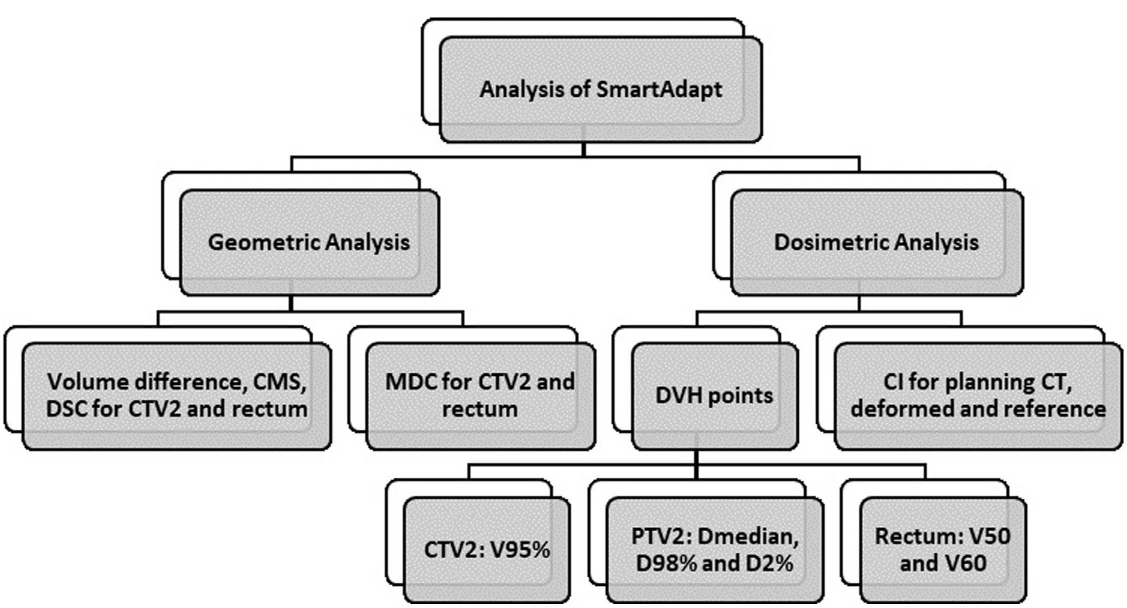

Fig. 1. Diagram showing an overview of the methods used in this study to assess the performance of SmartAdapt.

was added isotropically to the CTV1 to create PTV1 and a 3 mm margin to the CTV2 to create PTV2. The bladder, femoral heads and the rectum (from the anus to the recto-sigmoid junction) were delineated. RapidArc plans were generated by the dosimetrist using inverse planning in Eclipse treatment planning system (Varian Medical Systems Inc, Palo Alto, CA). The Analytical Anisotropic Algorithm (AAA), which is a convolution-superposition algorithm available in Eclipse, was used for the dose calculation. Treatment was delivered using Varian Clinac iX with RapidArc. Varian Clinac iXs are equipped with on-board imaging system capable of performing CBCT. Prior to daily treatment delivery, CBCT images of the pelvic area were acquired and compared to planning CT images using soft-tissue matching to ensure that the prostate and the seminal vesicles were included in the PTV1. In accordance with imaging protocol, all matching was independently checked offline by a radiographer. CBCT images were stored in Eclipse. The CTV2 (prostate only) and the rectum (from the anus to the recto-sigmoid flexure) were contoured on CBCTs for fractions 1, 6, 11, 16, 21, 26 and 31 by the clinician.

It is worth pointing out that CT and CBCT have definitive limitations in the outlining of prostate CTVs. Our department now performs MRI image registration on most, if not all, radical prostate cases to assist in accurate target delineation. However, at the time this study was conducted this was not routine practice. The aim of this study was to assess the feasibility of using daily positional information from CBCT scans to guide plan adaptation. MRI fusion used to assist delineation of the original planning contours would not change the workflow or the results of the comparison.

In this study, for each fraction available the planning CT image with volumes and structures (source image) was registered to the CBCT image (target image) using SmartAdapt. First of all, a rigid registration was performed between the planning CT and the CBCT to bring the volumes and structures of both images into the same coordinate system. Following the rigid registration, the automatic deformable registration was carried out. The deformed image dataset was then exported. In SmartAdapt, the deformed image dataset, including structure set, was imported. This step was necessary to allow proper assessment of the contours from multiple deformed image datasets. The deformed image dataset was shown as registered to the planning CT and CBCT images.

For evaluating the performance of SmartAdapt, the manually-delineated contours on the CBCT images (reference) were propagated from the CBCT images to the deformed images to enable comparison (Fig. 2). Inter-observer variability in manual contouring was eliminated in this study because all the delineations were performed by the same clinical oncologist. Delineations of volumes and structures for each patient were performed according to clinical protocol. It was not possible to exclude intra-observer variability.

2.1. Geometric analysis

Although various evaluation metrics have been proposed in the literature to quantify the agreement between contours, there is no widely accepted method for geometrical comparison [15]. The statistic tool in SmartAdapt was used to compare volumes, centre of mass shifts (CMS) and Dice Similarity coefficient (DSC) between relevant contours for both rigid and deformable registration.

Volume measurement comparison is a simple method for reporting geometrical differences between contours; however, it does not provide information on positional change. A CMS analysis can be useful for describing displacements of two structure or volumes. The CMS is given by the following expression: [9]

$$CMS = \sqrt{X_{CMS}^2 + Y_{CMS}^2 + Z_{CMS}^2}$$

Equation 1. Centre of mass shift (CMS)

Where X_{CMS}, Y_{CMS} and Z_{CMS} are the displacements in the X, Y and Z direction respectively. CMS has the drawback that it does not take differences in shape into account. To overcome this problem, overlap-based metrics are used. The DSC is a measure of spatial overlap and is given by the following expression: [9,16]

$$DSC = \frac{2(V_{RIG,\ DIR} \cap V_{REF})}{V_{RIG,\ DIR} + V_{REF}}$$

Equation 2. Dice Similarity coefficient (DSC)

Where $V_{RIG,DIR}$ are the rigidly and deformed registered structure volumes and V_{REF} are the corresponding structure volumes on the reference image. DSC values can range between 0 (no overlap) and 1 (perfect overlap of contours). A DSC greater than 0.70 can be considered acceptable for prostate cancer [17]. The main advantage of using DSC is that it is easy to visualise. However, one major drawback is that it is based on spatial overlap of voxels regardless to their distance to the reference contour. DSC fails to provide information on the directionality of the error detected. To overcome this problem, distance-based metrics have been developed. The mean distance to conformity metric (MDC), introduced by Jena et al. [18], provides information of the changes in position of the contour pairs under investigation. MDC is defined as the mean distance of each outlying voxel from the reference contour to the evaluation contour. MDC is given by the following expression:

$$MDC = \frac{1}{N(A)} \sum_{i=0}^{N(A)} d(A_i, B_i)$$

Equation 3. Mean Distance to Conformity (MDC)

Where $d\ (A_i,B_i)$ is the distance from point i on surface A to the closest point on surface B, and $N(A)$ is the total number of surface points on contour A. The advantage of using MDC is that it provides additional information on the shape difference between the evaluation and the reference contour. MDC is not supplied by SmartAdapt. In this study, SHERRI (Surrey Heuristic Engine for Radiotherapy, Radiobiology and Imaging), developed by Dr Jena, was used to measure MDC and evaluate the performance of SmartAdapt DIR. In general, an MDC value of less than 2 mm can be considered acceptable [18].

2.2. Dosimetric analysis

Firstly, a rigid registration between the deformed image (source image) for the first fraction and the original planning CT image dataset (target image) was carried out to bring the volumes and structures of both images into the same coordinate system. The deformed CTV2 and rectum were then propagated from the smartadapted deformed image to the original planning CT.

In Eclipse, a new course was created. The original treatment plan was copied and pasted, assigning the new structure set that contains the original and the deformed contours, as well as the reference contours generated by the clinician on the CBCT images. The reference contours were propagated for the geometric analysis. The new treatment plan was re-calculated with the same settings, including the same number of monitor units (MUs) as in the original plan (Fig. 3). The new dose distribution can then be analysed in plan evaluation. As in Maund et al. [14], it is assumed that the original dose distribution is spatially invariant. For deep-seated tumours such as the prostate, this assumption can be considered reasonable.

For the dosimetric analysis, the change in plan metrics on the manually-delineated CBCT contours by the clinician (reference) will be compared against the change in plan metrics observed when using SmartAdapt. Several DVH points were chosen. To evaluate the dose coverage to the PTV2, the D_{median} (dose received

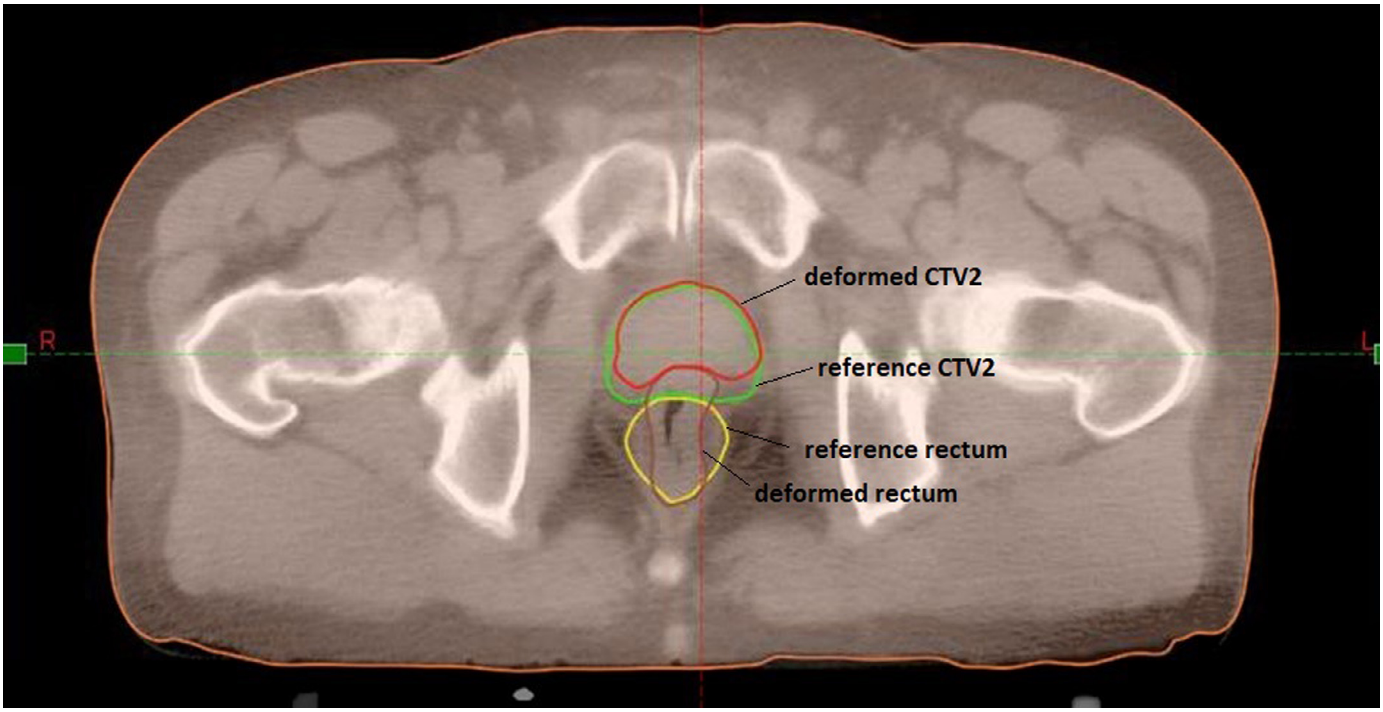

Fig. 2. Example of deformable image registration using patient 18, showing deformed CTV2 in red, reference CTV2 in green, deformed rectum in brown and reference rectum in yellow. (For interpretation of the references to color in this figure legend, the reader is referred to the web version of this article.)

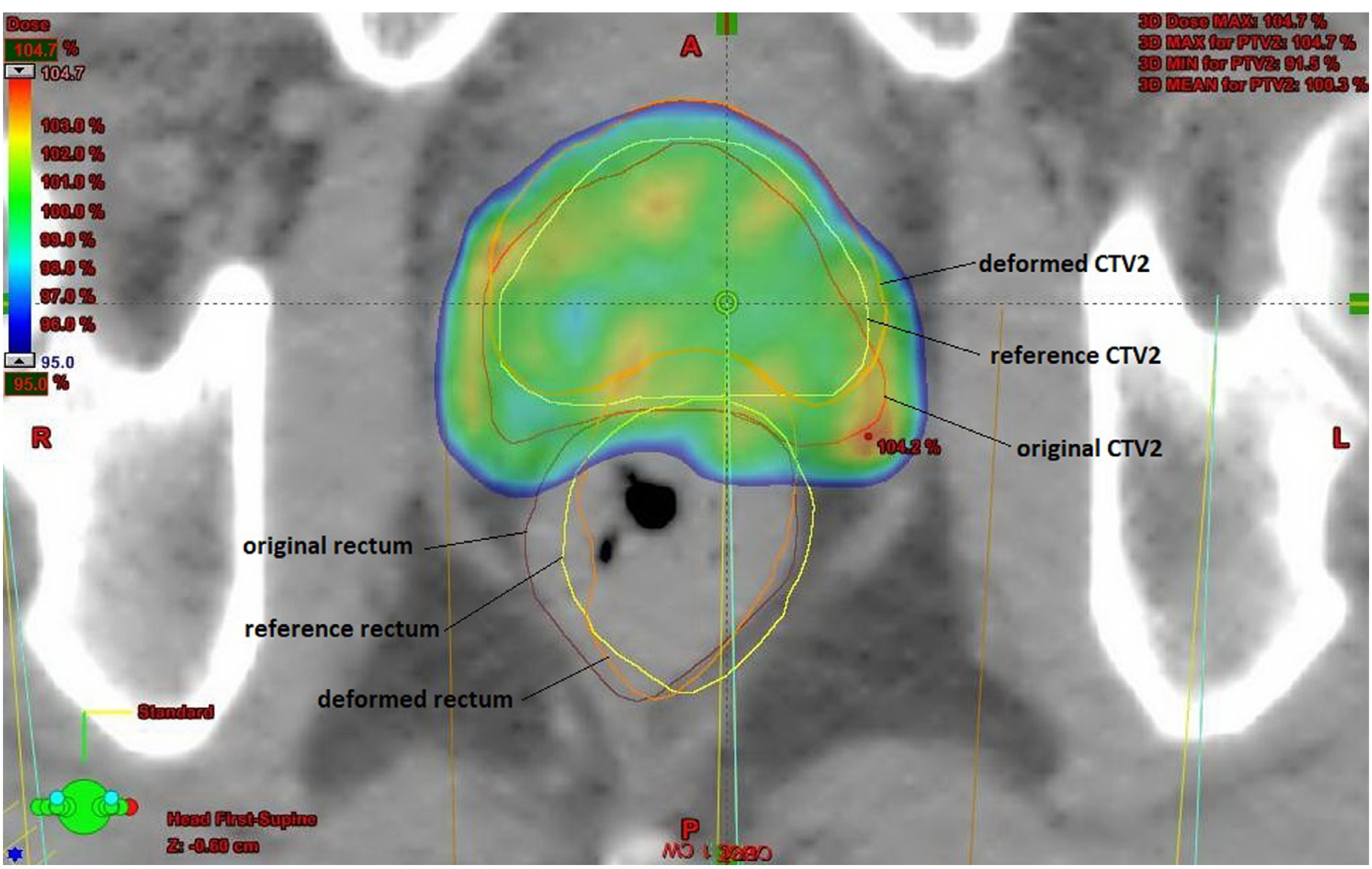

Fig. 3. Treatment plan for patient 18, as an example, showing the V95%, the original CTV2 in red, the deformed CTV2 in orange, the reference CTV2 in yellow, the original rectum in brown, the deformed rectum in orange and the reference rectum in yellow. (For interpretation of the references to color in this figure legend, the reader is referred to the web version of this article.)

by 50% of the PTV2 volume), $D_{98\%}$ (dose to 98% of the volume) and $D_{2\%}$ (dose to 2% of the volume) were determined, as recommended by ICRU Report 83 [19]. The absorbed dose to the rectum was determined by V_{50} and V_{60}, which are the percentages of rectal volume receiving 50 Gy and 60 Gy respectively. These points were selected based on the results of Fiorino et al. [20], which suggest that V_{50} below 60–65% and V_{60} below 50–55% are robust cut-off values for late rectal toxicity.

DVHs, however, present some limitations. For example, they do not provide spatial information, their interpretation is subjective, and the implications of small differences are not well understood. For this reason, in addition to the DVH points, the conformity index (CI), which was introduced in ICRU Report 62 [21], was determined to assess whether the treated volume encompasses the PTV, indicating plan conformity. A CI value equal to one corresponds to ideal conformation. The CI is given by the following expression: [22]

$$CI = \frac{V_{95\%}}{PTV\ Volume}$$

Equation 4. Conformity Index (CI)

Where $V_{95\%}$ is the volume within the patient receiving at least 95% of the prescribed dose. Although the CI is very easy to calculate, it is not an ideal evaluation metric since it fails to take into consideration the degree of spatial intersection or the shapes of the two volumes of interest [22]. Furthermore, the PTV is a geometrical concept design to ensure that the CTV received an adequate absorbed dose. The CTV to PTV margin is not modelled by SmartAdapt. For this reason, to analyse the performance of SmartAdapt, it was decided to create a deformed PTV2 by extending the deformed CTV2 by a margin of 0.3 cm isotropically, using the tools in Eclipse. The reference CTV2 was also extended by 0.3 cm isotropically to create the reference PTV2. This is in accordance with departmental protocol for prostate cancer.

3. Results

3.1. Geometric analysis

Statistical analysis of the evaluation metrics was performed using IBM SPSS Statistics Version 20. Data were found to be normally distributed. For the 18 patients, the mean and standard deviation values of the evaluation metrics were calculated. A paired *t*-test was carried out to determine whether the evaluation metrics were statistically different between rigid and deformable registration. The statistical significance was set at 0.05.

The results are shown in Table 1. For both CTV2 and rectum the *p*-values for CMS and DSC are less than 0.05. In some cases, DIR resulted in worse evaluation metrics for CTV2 and rectum than using rigid registration alone.

Considerable variation in the rectal volume between patients for rigid and DIR can be observed, indicating that using the difference in volume between contours alone is not a good evaluation metric for assessing the performance of SmartAdapt. Figs. 4 and 5 show the CTV2 and the rectal volume difference between the deformed and the reference contours for the 18 patients, respectively.

3.2. Results of mean distance to conformity for deformable registration

The MDC is the average distance that all the outlying points in the deformed contours must be moved in 3D to achieve conformity with the manually-delineated contours on the CBCT images [18]. The MDC consists of an over-contouring component, where the deformed contours extend beyond the reference contours, and an under-contouring component, where the deformed contours are smaller than the reference contours. The results of MDC, Over-contour and Under-contour in mm for DIR (using manual contours on CBCT images as reference), provided by SHERRI, were recorded on SPSS. The data were found to be normally distributed. For the 18 patients, the mean and standard deviation values of MDC, Over-contour and Under-contour were calculated for CTV2 and rectum. The results are shown in Table 2.

In general, the MDC values for rectum were higher than those for the CTV2. For one patient a MDC for rectum of 4.42 mm between the deformed and the planning CT contour was recorded in fraction 21, which could be caused by the DIR not being able to compensate for rectal volume changes between the planning CT and the CBCT. The mean value of MDC for CTV2, which is less than 2 mm, can be considered acceptable. From the results, it can also be noted that in general, SmartAdapt tends to under-contour the structures/volumes.

3.3. Dosimetric analysis

The difference in DVH points for the original planning CT and the deformed volumes/structures relative to the reference were determined. The results were expressed as a percentage.

As can be seen from Table 3, the difference in the DVH points relative to the reference were larger for the rectum than for the CTV2 and the PTV2. For the PTV2, the median percentage difference in DVH points was within 1.6%, indicating similar target coverage for all datasets. However, differences of up to 22% on the deformed PTV2 relative to the reference were observed.

In addition to the DVH points, the CI was determined to evaluate the coverage of the original planning CT, deformed and reference PTV2. Table 4 shows the results for the CI using the original plan. As explained, the CI was determined by calculating the ratio of the volume within the patient covered by the 95% isodose in cm^3 to the total volume of PTV2 (original planning CT, deformed by SmartAdapt or reference) in cm^3.

The median values of CI vary depending on the PTV2 volume used. The median CI value for the original PTV2 is very close to one. The median CI value for the reference is higher than the values for the deformed and the original PTV2. The median CI values for the deformed and the reference PTV2 were similar, indicating similar target coverage. These values are also higher than one, indicating that healthy tissue is included in the 95% isodose.

Table 1
Comparison of evaluation metrics between rigid and deformable registration, showing mean±standard deviation.

Structure/ Volume	Metric	Rigid	Deformable	*p*-value
CTV2 (prostate only)	Volume Difference (cm^3)	3.0 ± 4.4	1.9 ± 7.1	0.107
	CMS (cm)	0.26 ± 0.19	0.35 ± 0.20	<0.001
	DSC	0.85 ± 0.06	0.81 ± 0.06	<0.001
Rectum	Volume Difference (cm^3)	3.8 ± 26.2	5.1 ± 20.4	0.393
	CMS (cm)	0.96 ± 0.48	0.81 ± 0.46	0.022
	DSC	0.67 ± 0.08	0.69 ± 0.08	<0.001

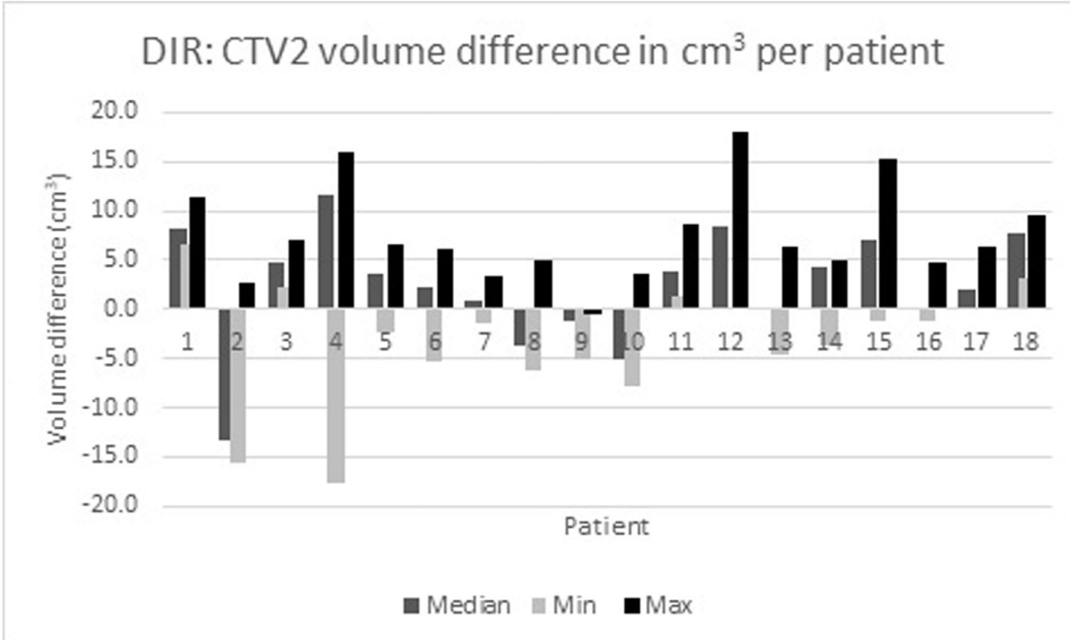

Fig. 4. Volume difference between the deformed and the reference CTV2 in cm^3 per patient, showing the median, minimum and maximum values.

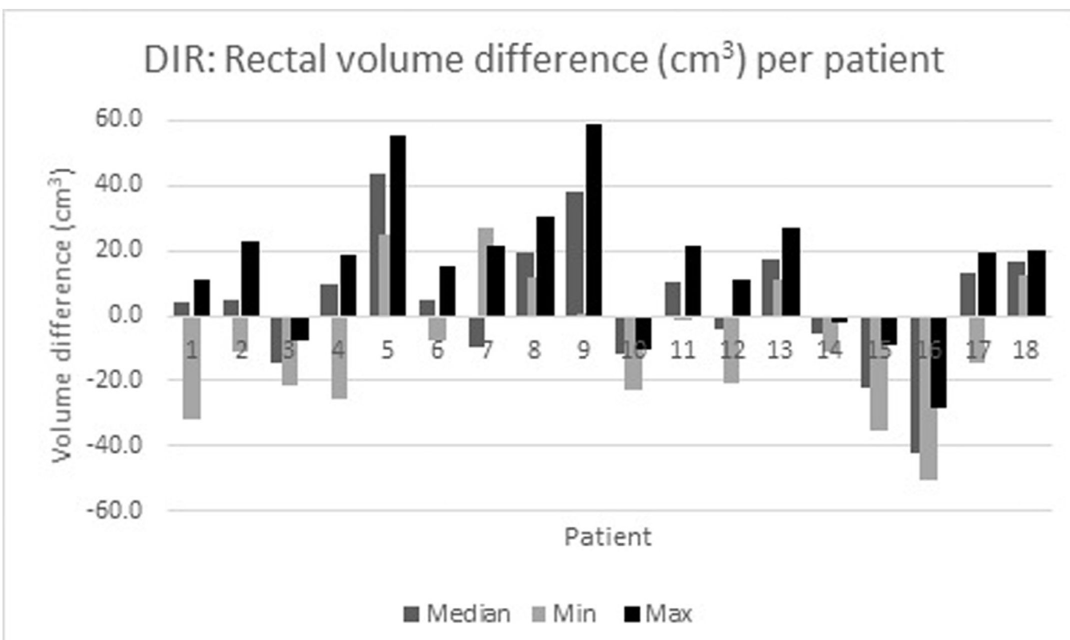

Fig. 5. Volume difference between the deformed and the reference rectum in cm^3 per patient, showing the median, minimum and maximum values.

Table 2
MDC, Over-contour and Under-contour results, showing mean ± standard deviation.

Structure/Volume	MDC (mm)	Over-contour (mm)	Under-contour (mm)
CTV2 (prostate only)	1.54 ± 0.76	0.68 ± 0.53	0.86 ± 0.65
Rectum	2.68 ± 1.17	1.10 ± 0.55	1.58 ± 1.15

4. Discussion

4.1. Geometric analysis

The main weakness of the method used in our geometric evaluation is that it includes intra-observer variability. Due to the noise and low contrast in CBCT images, it can be challenging for the clinical oncologist to draw the contours consistently. Although manual contours by an expert are considered the gold standard, these contours are not guaranteed to be correct due to human factors contributing to the assessment of the images.

As can be seen in Table 1, in general, the results obtained for the CTV2 are better than the results for rectum for both rigid and DIR. This was also found by Thor et al. [23]. This study uses

Table 3
Difference in the DVH points between planning CT or deformed volumes/structures and reference. Difference relative to the reference expressed as a percentage and presented as median and range between brackets.

Volume/Structure	DVH point	Difference between planning CT and reference	Difference between deformed and reference
CTV2 (prostate only)	$V_{95\%}$	0.0 (0.0, 3.8)	0.0 (−4.4, 3.8)
PTV2 (CTV2 + 0.3 cm isotropically)	D_{median}	−0.2 (−0.3, 0.1)	0.3 (0.1, 0.5)
	$D_{98\%}$	−1.6 (−3.2, 17.9)	−0.5 (−1.5, 22.0)
	$D_{2\%}$	0.0 (−0.1, 0.4)	0.4 (0.2, 0.7)
Rectum	V_{50}	−20.8 (−55.1, 86.4)	−9.7 (−47.2, 77.1)
	V_{60}	−25.1 (−64.6, 138.4)	−2.2 (−50.5, 141.7)

Table 4
Results of CI, showing the median value followed by the range between brackets.

CI (planning CT)	CI (deformed)	CI (reference)
1.05 (0.99, 1.08)	1.40 (1.23, 1.84)	1.45 (1.29, 1.86)

5 prostate patients to assess the performance of a DIR tool for contour propagation from CT to CBCT scans in prostate cancer. However, the study only uses the DSC as evaluation metric and a qualitative visual scoring by a clinician. Furthermore, the study does not include a dosimetric analysis.

It can be noted that DIR sometimes resulted in worse evaluation metrics compared to rigid registration alone. This result was also observed in the geometrical evaluation of lung cancer patients performed by Ottosson et al. [16]. For CTV2 and rectum there is a difference in CMS and DSC between rigid and deformable registration. This can be due to objects present in one image but not in the other which can cause problems for the Demons algorithm used in SmartAdapt, leading to incorrect transformations. Another difficulty could be the poorer image quality of CBCT images compared to CT images, which could make DIR difficult. Compared with CT, CBCT images have inferior contrast resolution, decreased accuracy in CT numbers and increased image artifacts [24]. Thor et al. [23] suggested that the performance of the Demons algorithm could be improved by increasing the CBCT image quality. Acquisition parameters for CBCT, such as tube voltage, collimation, filter type, half or full fan mode, affect the image quality [5]. The amount of scatter and artifacts are also affected by patient size. However, improving image quality could potentially increase concomitant imaging dose to the patient. Radiation dose from pelvic CBCT depends on several factors such as beam quality, tube output, scanning geometry, technique setting and patient size [14]. At our hospital, the estimated dose to the isocentre is approximately 25 mGy per standard pelvic CBCT scan [14]. CBCT imaging dose contributes to the treatment dose and could potentially increase the risk of developing second cancers. Any additional radiation dose needs to be justified in terms of patient benefit. It is worth mentioning that testing altered CBCT acquisition protocols, increasing dose to improve image quality, would significantly alter design and ethical implications of this study, and it is outside the scope of this manuscript.

Analysing the results obtained for the mean MDC, Over-contour and Under-contour for DIR of planning CT to CBCT images (Table 2), using the manually-drawn contours on CBCT images as reference, we can see that in general, SmartAdapt tends to undercontour the CTV2 and the rectum. The results for the CTV2 are better than those for the rectum. The mean MDC (mm) for the CTV2 was less than 2 mm, which can be considered acceptable as indicated by Jena et al. [18].

One limitation shared by all evaluation metrics used in this geometric evaluation is the lack of connexion between the quantification of geometrical error of DIR and the effect that error has on the dose distribution [25]. Wu et al. [26] showed that geometric and dosimetic evaluations are related, but not equivalent. Furthermore, Voet et al. [17] found that DSC is not an indicator of dosimetric agreement. For this reason, a dosimetric analysis was performed as part of this study.

4.2. Dosimetric analysis

To our knowledge the method used for this dosimetric analysis is novel and allows the comparison of the absorbed doses to the PTV2 and rectum between the original planning, the deformed and the reference volumes/structures. The aim of this dosimetric analysis was to determine whether SmartAdapt enables us to make the same judgements on the impact of anatomical changes that by manually re-outlining the volumes and structures. For this purpose, the deformed volumes/structures were propagated to the original planning CT dataset and the initial treatment plan was recalculated using the same settings and number of MUs. DVH points were determined to compare the absorbed doses to the CTV2, PTV2 and the rectum, using the original planning CT, the deformed and the reference volumes/structures. A weakness of this method, however, is that it assumes that the treatment plan has not changed. The method assumes that small changes in patient position and contour do not significantly affect the calculated dose at depth in the patient. This is called shift invariance [27]. This assumption is reasonable as long as the prostate patients do not lose or gain significant weight.

To date, most studies that evaluate the performance of SmartAdapt or other DIR algorithms are limited to head and neck. Eiland et al. [9] performed a geometric and dosimetric analysis of SmartAdapt for adaptive radiotherapy in head and neck IMRT. The study used 7 patients, each with a planning CT, a CBCT and a re-scanning CT. The manually-delineated structures/volumes by the clinician on the re-scanning CT were used as reference. A rigid registration followed by a deformable registration was performed between the planning CT and the CBCT images. The original plan was copied and pasted to the re-scanning CT and the deformed image. The plan was then re-calculated using the same settings and the same number of MUs as the original plan. D_{median}, $D_{98\%}$ and $D_{2\%}$ were determined to evaluate the dose coverage to the CTV. In our opinion, the main weakness of this method is that it uses the re-scanning CT as reference. The re-scanning CT was acquired at a different time than the CBCT and would fail to account for anatomical changes during the course of treatment. Although, this method can be justified in the case of head and neck, it would not be a valid method for assessing the performance of SmartAdapt, in terms of dosimetry, for prostate cancer due to inter-fractional motion. In the case of head and neck, the parotid glands, are known to change volume during a course of radiotherapy treatment [28]. The parotid volume change can be measured on a daily or weekly timescale. The re-scan CT would give similar information to a CBCT scan acquired within one or two days. The method, however, would not be adequate for short-term changes or for assessing the effect of daily motion on the dose to organs at risk. Eiland et al. [9] suggested that the deformed dataset produced by SmartAdapt could be used as a decision tool to establish whether the patient would need to be rescanned. In order to implement this clinically, the deformed dataset should overestimate the need for re-planning.

In our study, the DVH points of V_{50} and V_{60} had different values for the deformed and the planning CT rectum, indicating that the positions of this organ in relation to the reference rectum (manually-drawn contour on the CBCT image dataset) were different. This can be explained by rectal volume changes shifting the rectum into an area of lower or higher dose. The dosimetric changes for the rectum relative to the reference appear worse on the planning CT than on the deformed structure, indicating that the deformed rectum underestimated the need for replanning. For the target volumes, the median percentage differences in DVH points between the planning CT and the deformed volume relative to the reference volume were within 1.6%, which indicates that the original plan is very robust and can provide reasonable target coverage despite the anatomical changes. However, for the CTV2, differences of up to 4.4% in $V_{95\%}$ were observed between the deformed and the reference. For the PTV2, differences of up to 22% in $D_{98\%}$ were observed between the deformed and the reference. Larger differences in range were found between the deformed and the reference PTV2 than the planning CT and the reference PTV2, which overestimate the need for re-planning. If the deformed PTV2 were to be used as a decision tool for when to consider re-planning, then this would be acceptable.

The median values for the CI obtained from the deformed PTV2 and reference PTV2 were higher than those obtained from the planning CT PTV2, indicating that more healthy tissue was being included in the high dose region. Median values for the CI from the deformed PTV2 were generally lower than, or very close to, those obtained from the reference PTV2. The median value for the CI using the original PTV2 is very close to one, indicating very good conformation. This was expected since the treatment plan was optimised to the original planning CT structure set. The results of CI using the deformed PTV2 are very similar to those using the reference PTV2, which can suggest that this conformity measure could be used as an indicator for re-planning. However, these results need to be interpreted with care. The CI does not consider the location of the prescription isodose volume relative to the target volume. This means that in some circumstances the CI can give false perfect scores on a non-conformal plan. Paddick[29] published a literature review on scoring ratios to determine the conformity of radiosurgical plans and gave various examples of volumes of interest which would result in a CI of 1, even though they did not present ideal conformation, showing that the CI does not account for the relative positions of the two volumes of interest. The CI has the advantage that it is easy to calculate and can be used to compare two treatment plans, but should not be used in isolation as a decision tool.

5. Conclusion

SmartAdapt has the potential of facilitating adaptive planning of prostate RapidArc. For both rigid and deformable registration, the results of the evaluation metrics for the CTV2 are generally better than those for the rectum. The results obtained in the geometric evaluation suggest that the deformed structures/volumes produced by SmartAdapt are not able to replace manual contouring by the clinician completely. However, as suggested by Chao et al. [30]; Hou et al. [12] and Eiland et al. [9], they could be used as a helpful tool to assist the clinician with the manual contouring of volumes/structures on the re-scanning planning CT. Ramadaan et al. [31] found that SmartAdapt could save considerable time in re-contouring head and neck structures on re-scanning CTs. However, the study also recommended careful review of the deformed structures generated by SmartAdapt.

The difference in DVH points between the deformed and the reference CTV2 and PTV2 was worse than the difference between the planning CT and the reference, overestimating the need for re-planning. However, there was a tendency for the deformed rectum to underestimate the need for re-planning, when compared to the reference rectum (manually-drawn contours on the CBCT image dataset). The CI values obtained from the deformed PTV2 are very similar to those from the reference PTV2. Thus, in combination with the CI from the PTV2, the deformed CTV2 and PTV2 could be used to evaluate whether a rescan is needed when disregarding the deformed rectum. All re-scans would need to be authorised by the clinical oncologist under the Ionising Radiation (Medical Exposure) Regulations 2000 [32] and the benefits of re-scanning and re-planning should outweigh the risks.

It is worth pointing out that as shown by Yip et al. [28], not all patients would benefit from adaptive radiotherapy. Moreover, this strategy could be time-consuming. Therefore, it would be recommended to identify patients who will benefit from adaptive radiotherapy, improving tumour control probability whilst reducing normal tissue complications.

At our hospital, after cautious analysis of the results obtained in this study, it has been decided not to implement SmartAdapt clinically to trigger adaptive decisions in prostate cancer. Due to the limitations described in this study, it has been decided that SmartAdapt is not a robust tool to be used routinely. However, SmartAdapt can be a useful tool in assisting the clinician with delineation on the re-scanning CT rather than starting from scratch, potentially saving time spent on manual delineation. It can also be a useful tool in generating evaluation metrics such as Volume Difference, CMS and DSC between evaluation and reference contours. The results of these evaluation metrics could be used for the quality assessment of contouring and as an educational tool for clinicians learning how to delineate.

Acknowledgments

We wish to confirm that there are no known conflicts of interest associated with this manuscript and there has been no significant financial support for this work that could have influenced its outcome. The research did not receive any specific grant from funding agencies in the public, commercial, or not-for-profit sectors.

We can confirm that HRA and HCRW Approval was given (IRAS project ID: 253822) and that the patients undergoing treatment gave their informed consent to the collection and use of data for research purposes.

References

[1] Scaife JE, Thomas SJ, Harrison K, Romanchikova M, Sutcliffe MPF, Forman JR, et al. Accumulated dose to the rectum, measured using dose-volume histograms and dose-surface maps, is different from planned dose in all patients treated with radiotherapy for prostate cancer. Br J Radiol 2015;88:20150243. doi:10.1259/bjr.20150243.

[2] Cancer research UK, Prostate cancer incidence statistics, available from http://www.cancerresearchuk.org/cancer-info/cancerstats/types/prostate/incidence/, 2016, [accessed July 2016].

[3] Otto K. Volumetric modulated arc therapy: IMRT in a single gantry arc. Med Phys 2008;35:310–17. doi:10.1118/1.2818738.

[4] Ghilezan M, Yan D, Martinez A. Adaptive Radiation Therapy for Prostate Cancer. Semin Radiat Oncol 2013;20:130–7. doi:10.1016/j.semradonc.2009.11.007.

[5] Richter A, Hu Q, Steglich D, Baier K, Wilbert J, Guckenberger M, et al. Investigation of the usability of conebeam CT data sets for dose calculation. Radiat Oncol 2008;3:42. doi:10.1186/1748-717X-3-42.

[6] Thirion JP. Image matching as a diffusion process: an analogy with Maxwell's demons. Med Image Anal 1998;2:243–60. doi:10.1016/S1361-8415(98)80022-4.

[7] Wang H, Dong L, Lii MF, Lee AL, De Crevoisier R, Mohan R, et al. Implementation and validation of a three-dimensional deformable registration algorithm for targeted prostate cancer radiotherapy. Int J Radiat Oncol Biol Phys 2005;61:725–35. doi:10.1016/j.ijrobp.2004.07.677.

[8] Wang H, Dong L, O'Daniel J, Mohan R, Garden AS, Ang KK, et al. Validation of an accelerated "demons" algorithm for deformable image registration in radiation therapy. Phys Med Biol 2005;50:2887–905. doi:10.1088/0031-9155/50/12/011.

[9] Eiland RB, Maare C, SjöStröm D, Samsøe E, Behrens CF. Dosimetric and geometric evaluation of the use of deformable image registration in adaptive intensity-modulated radiotherapy for head-and-neck cancer. J Radiat Res 2014;55:1002–8. doi:10.1093/jrr/rru044.

[10] Veiga C, McClelland J, Moinuddin S, Lourenço A, Ricketts K, Annkah J, et al. Toward adaptive radiotherapy for head and neck patients: feasibility study on using CT-to-CBCT deformable registration for "dose of the day" calculations. Med Phys 2014;41:31703. doi:10.1118/1.4864240.

[11] Tsuji SY, Hwang A, Weinberg V, Yom SS, Quivey JM, Xia P. Dosimetric evaluation of automatic segmentation for adaptive IMRT for head-and-neck cancer. Int J Radiat Oncol Biol Phys 2010;77:707–14. doi:10.1016/j.ijrobp.2009.06.012.

[12] Hou J, Guerrero M, Chen W, D'Souza WD. Deformable planning CT to cone-beam CT image registration in head-and-neck cancer. Med Phys 2011;38:2088–94. doi:10.1118/1.3554647.

[13] Pang PPE, Ong LKA, Ang KW, Master ZR, Tuan KLJ, Knight K, et al. EP-1636: Feasibility study of the use of SmartAdapt to evaluate the dosimetric impact of organ deformation in prostate case. Radiother Oncol 2015;115:S896–7. doi:10.1016/S0167-8140(15)41628-7.

[14] Maund IF, Benson RJ, Fairfoul J, Cook J, Huddart R, Poynter A. Image-guided radiotherapy of the prostate using daily CBCT: the feasibility and likely benefit of implementing a margin reduction. Br J Radiol 2014;87:1–10. doi:10.1259/bjr.20140459.

[15] Hanna GG, Hounsell AR, O'Sullivan JM. Geometrical analysis of radiotherapy target volume delineation: a systematic review of reported comparison methods. Clin Oncol 2010;22:515–25. doi:10.1016/j.clon.2010.05.006.

[16] Ottosson W, Lykkegaard Andersen Ja, Borrisova S, Mellemgaard a, Behrens CF. Deformable image registration for geometrical evaluation of DIBH radiotherapy treatment of lung cancer patients. J Phys: Conf Ser 2014;489:012077. doi:10.1088/1742-6596/489/1/012077.

[17] Voet PWJ, Dirkx MLP, Teguh DN, Hoogeman MS, Levendag PC, Heijmen BJM. Does atlas-based autosegmentation of neck levels require subsequent manual contour editing to avoid risk of severe target underdosage? A dosimetric analysis. Radiother Oncol 2011;98:373–7. doi:10.1016/j.radonc.2010.11.017.

[18] Jena R, Kirkby NF, Burton KE, Hoole ACF, Tan LT, Burnet NG. A novel algorithm for the morphometric assessment of radiotherapy treatment planning volumes. Br J Radiol 2010;83:44–51. doi:10.1259/bjr/27674581.

[19] Gregoire V, Mackie TR, de Neve W, Gospodarowicz M, Purdy JA, van Herk M, Miemierko A. ICRU Report 83: prescribing, recording, and reporting photon-beam Intensity-Modulated Radiation Therapy (IMRT). J ICRU 2010;10:1–106. doi:10.1093/jicru/10.1.Report83.

[20] Fiorino C, Cozzarini C, Vavassori V, Sanguineti G, Bianchi C, Mauro Cattaneo G, et al. Relationships between DVHs and late rectal bleeding after radiotherapy for prostate cancer: Analysis of a large group of patients pooled from three institutions. Radiother Oncol 2002;64:1–12. doi:10.1016/S0167-8140(02)00147-0.

[21] Landberg T, Chavaudura J, Dobbs J, Gerard JP, Hankd G, Horiot JC, Johansson KA, Möller T, Purdy J, Suntharalingam N, Svensson H. ICRU Report 62: prescribing, recording and reporting photon beam therapy (Supplement to ICRU report 50). J ICRU 1999:1–52 os32. doi:10.1093/jicru/os32.1.Report62.

[22] Feuvret L, Noël G, Mazeron JJ, Bey P. Conformity index: a review. Int J Radiat Oncol Biol Phys 2006;64:333–42. doi:10.1016/j.ijrobp.2005.09.028.

[23] Thor M, Petersen JBB, Bentzen L, Høyer M, Muren LP. Deformable image registration for contour propagation from CT to cone-beam CT scans in radiotherapy of prostate cancer. Acta Oncol (Madr) 2011;50:918–25. doi:10.3109/0284186X.2011.577806.

[24] Shaw CC. Cone beam computed tomography. Imaging in medical diagnosis and therapy series. Hendee WR, editor. CRC Press, Taylor & Francis Group; 2014. edited by.

[25] Pukala J, Johnson PB, Shah AP, Langen KM, Bova FJ, Staton RJ, et al. Benchmarking of five commercial deformable image registration algorithms for head and neck patients. J Appl Clin Med Phys 2016;17:25–40. doi:10.1120/JACMP.V17I3.5735.

[26] Wu Q, Ivaldi G, Liang J, Lockman D, Yan D, Martinez A. Geometric and dosimetric evaluations of an online image-guidance strategy for 3D-CRT of prostate cancer. Int J Radiat Oncol Biol Phys 2006;64:1596–609. doi:10.1016/j.ijrobp.2005.12.029.

[27] Craig T, Battista J, Van Dyk J. Limitations of a convolution method for modeling geometric uncertainties in radiation therapy. I. The effect of shift invariance. Med Phys 2003;30:2001–11. doi:10.1118/1.1589492.

[28] Yip C, Thomas C, Michaelidou A, James D, Lynn R, Lei M, et al. Co-registration of cone beam CT and planning CT in head and neck IMRT dose estimation: a feasible adaptive radiotherapy strategy. Br J Radiol 2014;87:20130532. doi:10.1259/bjr.20130532.

[29] Paddick I. A simple scoring ratio to index the conformity of radiosurgical treatment plans. J Neurosurg 2000;93(Suppl 3):219–22.

[30] Chao KSC, Bhide S, Chen H, Asper J, Bush S, Franklin G, et al. Reduce in variation and improve efficiency of target volume delineation by a computer-assisted system using a deformable image registration approach. Int J Radiat Oncol Biol Phys 2007;68:1512–21. doi:10.1016/j.ijrobp.2007.04.037.

[31] Ramadaan IS, Peick K, Hamilton DA, Evans J, Iupati D, Nicholson A, et al. Validation of Varian's SmartAdapt deformable image registration algorithm for clinical application. Radiat Oncol 2015;10(73). doi:10.1186/s13014-015-0372-1.

[32] Statutory Instruments 2000 No. 1059, Health and Safety, The Ionising Radiation (Medical Exposure) Regulations 2000, available from http://www.legislation.gov.uk/uksi/2000/1059/pdfs/uksi_20001059_en.pdf, [accessed July 2016].